Modeling of Improved Sine Trigonometric Single Valued Neutrosophic Information based Air Pollution Prediction Approach

Afrah Al-Bossly[1,*], Shoraim M. H. A.[2] , Amal O. A. Al magdashi [3], Badr Eldeen A. A. Abouzeed[4]

[1]Department of Mathematics, College of Science and Humanities in Al-Kharj, Prince Sattam Bin Abdulaziz University, Al-Kharj 11942, Saudi Arabia
[2]Department of Economics and Policy Sciences, College of Commerce and Economics, Hodeida University, Hodeida, Yemen.
[3]Department of Marketing and Production. Faculty of Administrative Sciences Thamar University, Yemen.
[4]Department of Economics, Faculty of Economics and Commercial, University of kordofan, Sudan
Emails: a.basli@psau.edu.sa; majedsh107@gmail.com; Amal.almaqdashi@tu.edu.ye; badralhaj2014@gmail.com

Abstract

Industrialization and urbanization air is getting polluted due to human activities. CO, NO, C6H6, etc., are the major air pollutants. The focus of air pollutants in ambient air is controlled by the climatological parameters including wind direction, atmospheric speed of wind, temperature, and humidity. Air pollution prediction is a critical sector where machine learning (ML) technique plays a major role. Its main purpose is to tackle and understand the damaging effects of air pollutants on the environment and human health. By using a range of ML techniques such as neural networks, regression, and decision trees, we could analyze historical data on air quality alongside geographical and meteorological factors. This allows us to design model that could detect patterns and predict pollution levels. By taking proactive measures such as providing timely alerts to the public, adjusting controls on emissions, and, implementing strategies to reduce pollution, we can work towards creating healthier and cleaner environments. Embracing the potential of artificial intelligence (AI) in air pollution prediction empowers us to protect the well-being of our communities and make informed decisions. Therefore, this study develops an Improved Sine Trigonometric Single Valued Neutrosophic Information based Air Pollution Prediction (ISTSVNI-APP) approach. The major objective of the ISTSVNI-APP technique is to exploit AI concepts with neutrosophic sets (NS) models for the forecasting of air pollution. To do so, the ISTSVNI-APP technique makes use of min-max normalization as the initial preprocessing step. For predicting air pollution, the ISTSVNI-APP technique uses STSVNI approach. To improve the performance of the ISTSVNI-APP technique, modified crow search algorithm (MCSA) is used for the parameter tuning of the STSVNI system. The performance evaluation of the ISTSVNI-APP method is verified utilizing benchmark dataset. The experimental outcomes stated that the ISTSVNI-APP technique gains better performance in predicting air pollution

Keywords: Artificial Intelligence; Air Pollution Prediction; Crow Search Algorithm; Neutrosophic Sets; Air Quality Index

1. Introduction

When a huge quantity of stuff like gases or any other particles from natural or other causes are combined in air, it generates pollution, therefore, it is called air pollution [1]. This enclosure into air generates various issues for living beings and some might main to demise which will decrease the amount of population. Pollutants inserted into air acquires three methods of substances [2]. The productions straight from the source inserted with air are called primary pollutants, where foundation of source can be procedure of normal resources. Vehicles on road and functioning trades produce their energy which mains to an upsurge in danger to persons by corrupting the atmosphere. Reaction amongst primary pollutants mains to secondary pollutants [3]. Oxidants from petrochemical

Doi: https://doi.org/10.54216/IJNS.240208
Received: December 29, 2023 Revised: February 19, 2024 Accepted: April 12, 2024

unit were known as secondary pollutants. An indicator is mainly created in order to analyze quality of air is known as Air quality index (AQI) [4]. Placing the level is very essential to preserve the dangerous persons from bare to the kinds of pollutants.

Artificial intelligence (AI) is the greatest technique where an element can sense, reason, create decisions, and adjust to its faults [5]. Machine Learning (ML) is a sub-section of AI that permits the element to be acquired without clearly being coded through a set of rules. Features or independent variables are inputs delivered to the system permitting it to take the association with the variable of interest [6]. The output to be assessed is known as an objective or reliant on variable. The features can be data of input itself, and few times novel features might be generated to deliver new suggestions for the algorithm to learn [7]. This idea of generating novel features with the aid of present features is termed feature engineering. ML technique is a process functional to the input data, which attempts to perceive its association with the value of target [8]. If the ML technique is recognized and novel hidden data (test data) is delivered to create forecasts, the level to which the forecasts resemble the test data denotes alteration. The technique is thought to be overfitting if it absorbs the training data to the amount that it negatively affects the performance of method on novel data [9]. Therefore, the objective of a technique is to contain lower bias and variance. The hyperparameters are the exterior configuration of the technique which can be altered to enhance the ML model, which diminishes the damage when functional to exact data [10].

This study develops an Improved Sine Trigonometric Single Valued Neutrosophic Information based Air Pollution Prediction (ISTSVNI-APP) approach. The main objective of the ISTSVNI-APP algorithm is to exploit AI concepts with neutrosophic sets (NS) models for the forecasting of air pollution. To do so, the ISTSVNI-APP technique makes use of min-max normalization as the initial preprocessing step. For predicting air pollution, the ISTSVNI-APP technique uses STSVNI approach. To improve the performance of the ISTSVNI-APP technique, modified crow search algorithm (MCSA) is utilized for hyperparameter tuning of the STSVNI methodology. The simulation evaluation of the ISTSVNI-APP algorithm has been verified by employing a benchmark database.

2. Related Works

Deepan and Saravanan [11] utilized a SARIMA technique for forecasting values signifying historical tendencies measured as seasonal patterns. Furthermore, a transductive LSTM (TLSTM) technique acquires dependences over recurrent memory blocks, so learning longer-term dependences for AQI forecast. Additionally, the TLSTM upsurges the precision near test points that establish a group of validation. Alkabbani et al. [12] present a complete model to estimate AQIs. At first, the work concentrated on forecasting hourly ambient focuses of PM2.5 and PM10 utilizing ANN. After the technique was proposed, this study paper has been protracted to the forecast of other standard pollutants, which served in the procedure of assessing AQI. The forecast of the AQI needs the range of a strong predicting technique, but also deeply trusts a series of pre-processing stages to pick analysts and grip dissimilar problems in data, with gaps. The projected technique was allocated with this by assigning lost entries utilizing missForest, an ML-based imputation model that used the RF model.

Anggraini et al. [13] main intention is to perfect the AQI for pollutants in the inclusive area utilizing distantly sensed information. To support this research, 425 data points from air pollution ranks spread universally are united utilizing ML Linear Regression techniques. Van et al. [14] projected a novel technique that unites (i) air pollution data processing methods and (ii) light-weight ML techniques to improve the AQI performance of forecasting. The three techniques such as DT, RF, and XGBoost, were equated through 3 estimation metrics such as MAE, RMSE, and R2 to suggest the finest technique in AQI forecast. In [15], an AQI forecast ANFIS system technique was formed using an already-existing dataset. In this case, the ANFIS model equates the performance of BPNN method, Gaussian-BNN, hybrid, and the Gaussian-hybrid BNN models.

Zhao et al. [16] main intention is to examine effect of these lockdowns on AQI utilizing a DL structure. Furthermore, to past pollutant attention and climatological features, we include social and spatial-temporal effects in the structure. Especially, spatial autocorrelation (SAC) unites time-based autocorrelation with spatial association. Abirami et al. [17] projected work to forecast AQI precisely by using the dataset on dissimilar ML technique with appropriate preprocessed model to discover elements of air suspensions for AQI value. In this paper, it is attempted to estimate the air condition in the limits of a definite area by employing ML plans.

3. The Proposed Method

In this paper, we have developed a novel ISTSVNI-APP system. The major intention of the ISTSVNI-APP technique is to exploit AI concepts with NS models for the forecasting of air pollution. It comprises three different procedures involving min-max normalization, STSVNI based air pollution prediction, and MCSA based parameter tuning. Fig. 1 illustrates the complete procedure of ISTSVNI-APP technique.

Doi: https://doi.org/10.54216/IJNS.240208
Received: December 29, 2023 Revised: February 19, 2024 Accepted: April 12, 2024

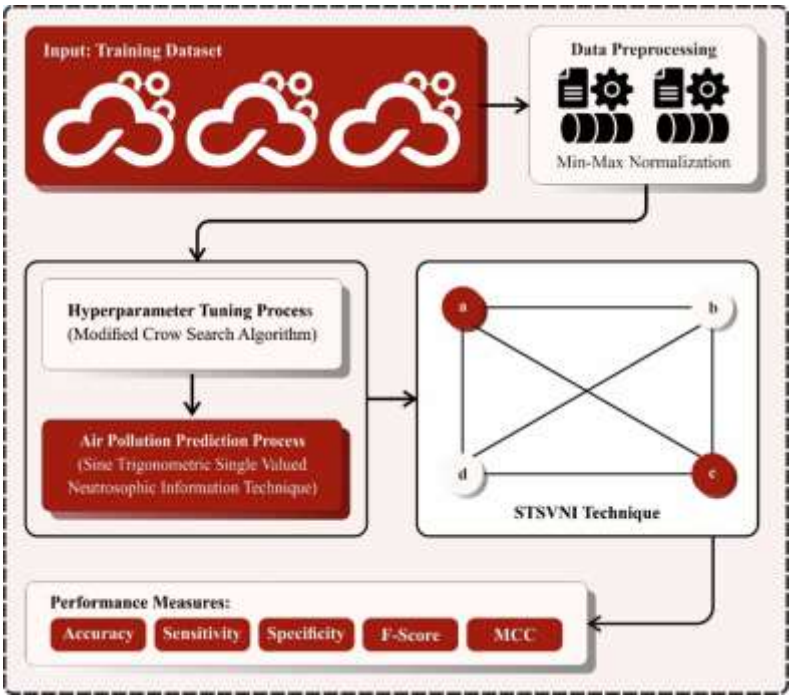

Figure 1: Overall process of ISTSVNI-APP model

A. Min-Max Normalization

At the initial preprocessing step, the ISTSVNI-APP technique makes use of min-max normalization. Min-max normalization (feature scaling) is a data preprocessing model which scales numerical characteristics within a certain specific range within (0, 1) [18]. This technique rescales all the features by subtracting the least values of the feature and then dividing by the variance between the lowest and highest values. Thereby, it preserves the relative relationships between the data points while ensuring that the feature is on a similar scale. Min-max normalization is specially tailored to data analysis and ML tasks where the models or algorithms utilized are sensitive to the scale of input feature. It makes interpretations easier, improves convergence rates, and avoids numerical instabilities.

B. Air Pollution Prediction using STSVNI

For predicting air pollution, the ISTSVNI-APP technique uses STSVNI approach. The new sine trigonometric hybrid AO on SVN dataset is given in this section [19].

Definition3.1. Consider $\mathcal{U}_\hbar = \{\tilde{\rho}_{\wp_\hbar}(\mathfrak{b}), \urcorner_{\wp_\hbar}(\mathfrak{b}), \tilde{n}_{\wp_\hbar}(\mathfrak{b})\} \in SVNN(\mathfrak{I})$ $(\hbar \in \mathbb{N})$. The trigonometric hybrid geometric weight, represented by the sine function, for $SVNN(\mathfrak{I})$ is AO was characterized as $ST-SVNHWA$ and defined by:

$$ST-SVNHWA(\mathcal{U}_1, \mathcal{U}_2, \dots, \mathcal{U}_n) = \sigma_1 \mathbb{sim}(\mathcal{U}'_{v(1)}) \oplus \sigma_2 \mathbb{sim}(\mathcal{U}'_{v(2)}) \dots \oplus \sigma_n \mathbb{sim}(\mathcal{U}'_{v(n)})$$

$$= \sum_{\hbar=1}^{n} \sigma_\hbar \, \mathbb{sim}(\mathcal{U}'_{v(\hbar)}),$$

Weight of $\mathcal{U}_\hbar$ was characterized as $\partial_\hbar(\hbar = 1,2, \dots, n)$ containing $\partial_\hbar \geq 0$ and $\sum_{\hbar=1}^{n} \partial_\hbar = 1$ and g^{th} largest weight rate is $\mathcal{U}'_{v(\hbar)}(\mathcal{U}'_{v(\hbar)} = n\partial_\hbar \mathcal{U}_{v(\hbar)} | \hbar = 1,2, \dots, n)$ and overall sequences $(v(1), v(2), v(3), \dots, v(n)$. As well, weight vector $\sigma = \sigma_\hbar(\hbar = 1,2, \dots, n)$ with $\sigma_\hbar \geq 0$ and $\sum_{\hbar=1}^{n} \sigma_\hbar = 1$.

Theorem3.2. Consider $\mathcal{U}_\hbar = \{\tilde{\rho}_{\wp_\hbar}(\mathfrak{b}), \urcorner_{\wp_\hbar}(\mathfrak{b}), \tilde{n}_{\wp_\hbar}(\mathfrak{b})\} \in SVNN(\mathfrak{I})$ $(\hbar \in \mathbb{N})$ and the weights of $\mathcal{U}_\hbar$ characterized as $(\partial_1, \partial_2, \dots, \partial_n)^T$ subjected to $\sum_{\hbar=1}^{n} \partial_\hbar = 1$. The $ST-SVNHWA\ AO$ is described by the mapping $G^n \to G$ with weight vector $\sigma_\hbar$ $(\hbar = 1,2, \dots, n)$ having $\sigma_\hbar \geq 0$ and $\sum_{\hbar=1}^{n} \sigma_\hbar = 1$:

$$ST-SVNHWA\ (\mathcal{U}_1, \mathcal{U}_2, \dots, \mathcal{U}_n) = \sum_{\hbar=1}^{n} \sigma_\hbar \ \mathbb{sim}(\mathcal{U}'_{v(\hbar)})$$

Doi: https://doi.org/10.54216/IJNS.240208
Received: December 29, 2023 Revised: February 19, 2024 Accepted: April 12, 2024

$$= \begin{pmatrix} 1 - \prod_{\hbar=1}^{n} \left(1 - \text{sim}\left(\frac{\pi}{2}\tilde{\rho}'_{\wp\upsilon(\hbar)}\right)\right)^{\sigma_\hbar}, \\ \prod_{\hbar=1}^{n} \left(1 - \text{sim}\left(\frac{\pi}{2}1 - \text{ד}'_{\wp\upsilon(\hbar)}\right)\right)^{\sigma_\hbar}, \\ \prod_{\hbar=1}^{n} \left(1 - \text{sim}\left(\frac{\pi}{2}1 - \tilde{n}'_{\wp\upsilon(\hbar)}\right)\right)^{\sigma_\hbar} \end{pmatrix} \quad (1)$$

Proof. By using mathematical induction on n.

$$ST - SVNHWA\ (\mathcal{U}_1, \mathcal{U}_2) = \sigma_1\ \text{sim}\ (\mathcal{U}'_{\upsilon(1)}) \oplus \sigma_2\ \text{sim}\ (\mathcal{U}'_{\upsilon(2)}).$$

$\text{sim}(\mathcal{U}_1)$ and $\text{sim}\ (\mathcal{U}_2)$ are SVNNs and thus $\sigma_1\ \text{sim}(\mathcal{U}'_{\upsilon(1)}) \oplus \sigma_2\ \text{sim}(\mathcal{U}'_{\upsilon(2)})$ is $SVNN$.

$$ST\text{—}SVNHWA\ (\mathcal{U}_1, \mathcal{U}_2)$$

$$= \sigma_1\ \text{sim}\ (\mathcal{U}'_{\upsilon(1)}) \oplus \sigma_2\ \text{sim}\ (\mathcal{U}'_{\upsilon(2)})$$

$$= \begin{pmatrix} 1 - \left(1 - \text{sim}\left(\frac{\pi}{2}\tilde{\rho}'_{\wp\upsilon(1)}\right)\right)^{\sigma_1}, \\ \left(1 - \text{sim}\left(\frac{\pi}{2}1 - \text{ד}'_{\wp\upsilon(1)}\right)\right)^{\sigma_1}, \\ \left(1 - \text{sim}\left(\frac{\pi}{2}1 - \tilde{n}'_{\wp\upsilon(1)}\right)\right)^{\sigma_1} \end{pmatrix} \oplus \begin{pmatrix} 1 - \left(1 - \text{sim}\left(\frac{\pi}{2}\tilde{\rho}'_{\wp\upsilon(2)}\right)\right)^{\sigma_2}, \\ \left(1 - \text{sim}\left(\frac{\pi}{2}1 - \text{ד}'_{\wp\upsilon(2)}\right)\right)^{\sigma_2}, \\ \left(1 - \text{sim}\left(\frac{\pi}{2}1 - \tilde{n}'_{\wp\upsilon(2)}\right)\right)^{\sigma_2} \end{pmatrix}$$

$$= \begin{pmatrix} 1 - \prod_{\hbar=1}^{2} \left(1 - \text{sim}\left(\frac{\pi}{2}\tilde{\rho}'_{\wp\upsilon(\hbar)}\right)\right)^{\sigma_\hbar}, \\ \prod_{\hbar=1}^{2} \left(1 - \text{sim}\left(\frac{\pi}{2}1 - \text{ד}'_{\wp\upsilon(\hbar)}\right)\right)^{\sigma_\hbar}, \\ \prod_{\hbar=1}^{2} \left(1 - \text{sim}\left(\frac{\pi}{2}1 - \tilde{\text{n}}'_{\wp\upsilon(\hbar)}\right)\right)^{\sigma_\hbar} \end{pmatrix}$$

$$\text{ST} - \text{SVNWA}\ (\mathcal{U}_1, \mathcal{U}_2, \ldots \mathcal{U}_\kappa) = \begin{pmatrix} 1 - \prod_{\hbar=1}^{\kappa} \left(1 - \text{sim}\left(\frac{\pi}{2}\tilde{\rho}'_{\wp\upsilon(\hbar)}\right)\right)^{\sigma_\hbar}, \\ \prod_{\hbar=1}^{\kappa} \left(1 - \text{sim}\left(\frac{\pi}{2}1 - \text{ד}'_{\wp\upsilon(\hbar)}\right)\right)^{\sigma_\hbar}, \\ \prod_{\hbar=1}^{\kappa} \left(1 - \text{sim}\left(\frac{\pi}{2}1 - \tilde{\text{n}}'_{\wp\upsilon(\hbar)}\right)\right)^{\sigma_\hbar} \end{pmatrix}$$

$$ST - SVNHWA\ (\mathcal{U}_1, \mathcal{U}_2, \ldots \mathcal{U}_{\kappa+1})$$

$$= \sum_{\hbar=1}^{\kappa} \sigma_\hbar\ \text{sim}\ (\mathcal{U}'_{\upsilon(\hbar)}) \oplus \sigma_{\kappa+1}\ \text{sim}\ (\mathcal{U}'_{\upsilon(\kappa+1)})$$

$$= \begin{pmatrix} 1 - \prod_{\hbar=1}^{\kappa} \left(1 - \text{sim}\left(\frac{\pi}{2}\tilde{\rho}'_{\wp\upsilon(\hbar)}\right)\right)^{\sigma_\hbar}, \\ \prod_{\hbar=1}^{\kappa} \left(1 - \text{sim}\left(\frac{\pi}{2}1 - \text{ד}'_{\wp\upsilon(\hbar)}\right)\right)^{\sigma_\hbar}, \\ \prod_{\hbar=1}^{\kappa} \left(1 - \text{sim}\left(\frac{\pi}{2}1 - \tilde{n}'_{\wp\upsilon(\hbar)}\right)\right)^{\sigma_\hbar} \end{pmatrix} \oplus \begin{pmatrix} 1 - \left(1 - \text{sim}\left(\frac{\pi}{2}\tilde{\rho}'_{\wp\upsilon(\kappa+1)}\right)\right)^{\sigma_{\kappa+1}}, \\ \left(1 - \text{sim}\left(\frac{\pi}{2}1 - \text{ד}'_{\wp\upsilon(\kappa+1)}\right)\right)^{\sigma_{\kappa+1}}, \\ \left(1 - \text{sim}\left(\frac{\pi}{2}1 - \tilde{n}'_{\wp\upsilon(\kappa+1)}\right)\right)^{\sigma_{\kappa+1}} \end{pmatrix}$$

Doi: https://doi.org/10.54216/IJNS.240208
Received: December 29, 2023 Revised: February 19, 2024 Accepted: April 12, 2024

$$= \begin{pmatrix} 1 - \prod_{\hbar=1}^{\kappa+1} \left(1 - \mathbb{sim}\left(\frac{\pi}{2}\tilde{\rho}'_{\wp v(\hbar)}\right)\right)^{\sigma_\hbar}, \\ \prod_{\hbar=1}^{\kappa+1} \left(1 - \mathbb{sim}\left(\frac{\pi}{2}1 - \beth'_{\wp v(\hbar)}\right)\right)^{\sigma_\hbar}, \\ \prod_{\hbar=1}^{\kappa+1} \left(1 - \mathbb{sim}\left(\frac{\pi}{2}1 - \tilde{n}'_{\wp v(\hbar)}\right)\right)^{\sigma_\hbar} \end{pmatrix}$$

that is, when $n = z + 1$, Therefore, Eq. (1)embraces for any n. The proof is accomplished.

(1) Consider $\mathcal{U}_\hbar = \{\tilde{\rho}_{\wp_\hbar}, \beth_{\wp_\hbar}, \tilde{n}_{\wp_\hbar}\} \in SVNN(\beth)(\hbar = 1,2,3,\dots,n)$ thus $\mathcal{U}_\hbar = \mathcal{U}$. If

$ST - SVNHWA(\mathcal{U}_1, \mathcal{U}_2, \dots, \mathcal{U}_n) = \mathbb{sim}(\mathcal{U})$.

(2) While, $\mathcal{U}_\hbar = \{\tilde{\rho}_{\wp_\hbar}, \beth_{\wp_\hbar}, \tilde{n}_{\wp_\hbar}\}$, $\mathcal{U}_\hbar^- = \{\mathbb{mim}(\tilde{\rho}_{\wp_\hbar}), \mathbb{max}(\beth_{\wp_\hbar}), \mathbb{max}(\tilde{n}_{\wp_\hbar})\}$ and $\mathcal{U}_\hbar^+ = \{\mathbb{max}(\tilde{\rho}_{\wp_\hbar}), \mathbb{mim}(\beth_{\wp_\hbar}), \mathbb{mim}(n_{\wp_\hbar})\} \in SVNN\ (\beth)\ (\hbar = 1,2,3,\dots,n)$. At that moment,

$\mathbb{sim}\ (\mathcal{U}_\hbar^-) \leq ST - SVNHWA\ (\mathcal{U}_1, \mathcal{U}_2, \dots, \mathcal{U}_n) \leq\ \mathbb{sim}\ (\mathcal{U}_\hbar^+)$.

(3) $Let \mathcal{U}_\hbar = \{\tilde{\rho}_{\wp_\hbar}, \beth_{\wp_\hbar}, \tilde{n}_{\wp_\hbar}\}$, $\mathcal{U}_\hbar^* = \{\tilde{\rho}^*_{\wp_\hbar}, \beth^*_{\wp_\hbar}, \tilde{n}^*_{\wp_\hbar}\} \in SVNN(\beth)\ (\hbar = 1,2,3,\dots,n)$. If $\tilde{\rho}_{\wp_\hbar} \leq \tilde{\rho}^*_{\wp_\hbar}$, $\beth_{\wp_\hbar} \leq \beth^*_{\wp_\hbar}$ and $\tilde{n}_{\wp_\hbar} \leq \tilde{n}^*_{\wp_\hbar}$, at that point

$ST - SVNHWA\ (\mathcal{U}_1, \mathcal{U}_2, \dots, \mathcal{U}_n) \leq ST - SVNHWA\ (\mathcal{U}_1^*, \mathcal{U}_2^*, \dots, \mathcal{U}_n^*)$.

Definition3.3. Consider $\mathcal{U}_\hbar = \{\tilde{\rho}_{\wp_\hbar}(\mathfrak{b}), \beth_{\wp_\hbar}(\mathfrak{b}), \tilde{n}_{\wp_\hbar}(\mathfrak{b})\} \in SVNN(\beth)\ (\hbar \in \mathbb{N})$. The trigonometric hybrid geometric weight, represented by the sine function, for $SVNN(\beth)$ is AO was characterized as $ST - SVNHWG$ and defined by:

$$ST - SVNHWG\ (\mathcal{U}_1, \mathcal{U}_2, \dots, \mathcal{U}_n) = (\mathbb{sim}\ (\mathcal{U}'_{v(1)}))^{\sigma_1} \otimes (\mathbb{sim}(\mathcal{U}'_{v(2)}))^{\sigma_2} \otimes \dots \otimes (\ \mathbb{sim}\ (\mathcal{U}'_{v(n)}))^{\sigma_n}$$

$$= \prod_{\hbar=1}^{n} (\ \mathbb{sim}(\mathcal{U}'_{v(\hbar)}))^{\sigma}\hbar$$

If weight of $\mathcal{U}_\hbar$ was characterized as $\partial_\hbar$ $(\hbar = 1,2,\dots,n)$ taking $\partial_\hbar \geq 0$ and $\sum_{\hbar=1}^{n} \partial_\hbar = 1$ and g^{th} value of weight is $\mathcal{U}'_{v(\hbar)}(\mathcal{U}'_{v(\hbar)} = n\partial_\hbar \mathcal{U}_{v(\hbar)} | \hbar = 1,2,\dots,n)$ through overall sequences $(v(1), v(2), v(3), \dots, v(n))$. Weighted vector $\sigma = \sigma_\hbar$ $(\hbar = 1,2,\dots,n)$ with $\sigma_\hbar \geq 0$ and $\sum_{\hbar=1}^{n} \sigma_\hbar = 1$.

Theorem3.4. Consider $\mathcal{U}_\hbar = \{\tilde{\rho}_{\wp_\hbar}(\mathfrak{b}), \beth_{\wp_\hbar}(\mathfrak{b}), \tilde{n}_{\wp_\hbar}(\mathfrak{b})\} \in SVNN(\beth)\ (\hbar \in \mathbb{N})$ and the weight of $\mathcal{U}_\hbar$ characterized as $(\partial_1, \partial_2, \dots, \partial_n)^T$ depending on $\sum_{\hbar=1}^{n} \partial_\hbar = 1$. The ST—SVNHWG AO is represented as mapping $G^n \to G$ with weight vector $\sigma_\hbar$ $(\hbar = 1,2,\dots,n)$ containing $\sigma_\hbar \geq 0$ and $\sum_{\hbar=1}^{n} \sigma_\hbar = 1$:

$$ST - SVNHWG\ (\mathcal{U}_1, \mathcal{U}_2, \dots, \mathcal{U}_n) = \prod_{\hbar=1}^{n} \left(\mathbb{sim}\ (\mathcal{U}'_{v(\hbar)})\right)^{\sigma_\hbar}$$

$$= \begin{pmatrix} \prod_{\hbar=1}^{n} \left(\mathbb{sim}\left(\frac{\pi}{2}\tilde{\rho}'_{\wp v(\hbar)}\right)\right)^{\sigma_\hbar}, \\ 1 - \prod_{\hbar=1}^{n} \left(\mathbb{sim}\left(\frac{\pi}{2}1 - \beth'_{\wp v(\hbar)}\right)\right)^{\sigma_\hbar}, \\ 1 - \prod_{\hbar=1}^{n} \left(\mathbb{sim}\left(\frac{\pi}{2}1 - \tilde{n}'_{\wp v(\hbar)}\right)\right)^{\sigma_\hbar} \end{pmatrix} \quad (2)$$

Proof. by utilizing mathematical induction on n

$$ST - SVNHWG\ (\mathcal{U}_1, \mathcal{U}_2) = \left(\mathbb{sim}\ (\mathcal{U}'_{v(1)})\right)^{\sigma_1} \oplus \left(\mathbb{sim}\ (\mathcal{U}'_{v(2)})\right)^{\sigma_2}.$$

Doi: https://doi.org/10.54216/IJNS.240208
Received: December 29, 2023 Revised: February 19, 2024 Accepted: April 12, 2024

Based on Definition2.9, $\mathbb{sim}(\mathcal{U}_1)$ and $\mathbb{sim}(\mathcal{U}_2)$ are SVNNs and thus $\sigma_1\left(\mathbb{sim}\left(\mathcal{U}'_{v(1)}\right)\right)^{\sigma_1} \oplus \sigma_2\left(\mathbb{sim}\left(\mathcal{U}'_{v(2)}\right)\right)^{\sigma_2}$ is also SVNN.

$$ST-SVNHWG\left(\mathcal{U}_1,\mathcal{U}_2\right) = \left(\mathbb{sim}\left(\mathcal{U}'_{v(1)}\right)\right)^{\sigma_1} \oplus \left(\mathbb{sim}\left(\mathcal{U}'_{v(2)}\right)\right)^{\sigma_2}$$

$$= \begin{pmatrix} \left(\mathbb{sim}\left(\frac{\pi}{2}\tilde{\rho}'_{\wp v(1)}\right)\right)^{\sigma_1}, \\ 1-\left(\mathbb{sim}\left(\frac{\pi}{2}1-\tau'_{\wp v(1)}\right)\right)^{\sigma_1}, \\ 1-\left(\mathbb{sim}\left(\frac{\pi}{2}1-\tilde{n}'_{\wp v(1)}\right)\right)^{\sigma_1} \end{pmatrix} \oplus \begin{pmatrix} \left(\mathbb{sim}\left(\frac{\pi}{2}\tilde{\rho}'_{\wp v(2)}\right)\right)^{\sigma_2}, \\ 1-\left(\mathbb{sim}\left(\frac{\pi}{2}1-\tau'_{\wp v(2)}\right)\right)^{\sigma_2}, \\ 1-\left(\mathbb{sim}\left(\frac{\pi}{2}1-\tilde{n}'_{\wp v(2)}\right)\right)^{\sigma_2} \end{pmatrix}$$

$$= \begin{pmatrix} \prod_{\hbar=1}^{2}\left(\mathbb{sim}\left(\frac{\pi}{2}\tilde{\rho}'_{\wp v(\hbar)}\right)\right)^{\sigma_\hbar}, \\ 1-\prod_{\hbar=1}^{2}\left(\mathbb{sim}\left(\frac{\pi}{2}1-\tau'_{\wp v(\hbar)}\right)\right)^{\sigma_\hbar}, \\ 1-\prod_{\hbar=1}^{2}\left(\mathbb{sim}\left(\frac{\pi}{2}1-\tilde{n}'_{\wp v(\hbar)}\right)\right)^{\sigma_\hbar} \end{pmatrix}$$

$$ST-SVNHWG\left(\mathcal{U}_1,\mathcal{U}_2,\ldots\mathcal{U}_\kappa\right) = \begin{pmatrix} \prod_{\hbar=1}^{\kappa}\left(\mathbb{sim}\left(\frac{\pi}{2}\tilde{\rho}'_{\wp v(\hbar)}\right)\right)^{\sigma_\hbar}, \\ 1-\prod_{\hbar=1}^{\kappa}\left(\mathbb{sim}\left(\frac{\pi}{2}1-\tau'_{\wp v(\hbar)}\right)\right)^{\sigma_\hbar}, \\ 1-\prod_{\hbar=1}^{\kappa}\left(\mathbb{sim}\left(\frac{\pi}{2}1-\tilde{n}'_{\wp v(\hbar)}\right)\right)^{\sigma_\hbar} \end{pmatrix}$$

$$ST-SVNHWG\left(\mathcal{U}_1,\mathcal{U}_2,\ldots\mathcal{U}_{\kappa+1}\right) = \sum_{\hbar=1}^{\kappa}\left(\mathbb{sim}\left(\mathcal{U}'_{v(\hbar)}\right)\right)^{\sigma_\hbar} \oplus \left(\mathbb{sim}\left(\mathcal{U}'_{v(1)}\right)\right)^{\sigma_{\kappa+1}}$$

$$= \begin{pmatrix} \prod_{\hbar=1}^{\kappa}\left(\mathbb{sim}\left(\frac{\pi}{2}\tilde{\rho}'_{\wp v(\hbar)}\right)\right)^{\sigma_\hbar}, \\ 1-\prod_{\hbar=1}^{\kappa}\left(\mathbb{sim}\left(\frac{\pi}{2}1-\tau'_{\wp v(\hbar)}\right)\right)^{\sigma_\hbar}, \\ 1-\prod_{\hbar=1}^{\kappa}\left(\mathbb{sim}\left(\frac{\pi}{2}1-\tilde{n}'_{\wp v(\hbar)}\right)\right)^{\sigma_\hbar} \end{pmatrix} \oplus \begin{pmatrix} \left(\mathbb{sim}\left(\frac{\pi}{2}\tilde{\rho}'_{\wp v(\kappa+1)}\right)\right)^{\sigma_{\kappa+1}}, \\ 1-\left(\mathbb{sim}\left(\frac{\pi}{2}1-\tau'_{\wp v(\kappa+1)}\right)\right)^{\sigma_{\kappa+1}}, \\ 1-\left(\mathbb{sim}\left(\frac{\pi}{2}1-\tilde{n}'_{\wp v(\kappa+1)}\right)\right)^{\sigma_{\kappa+1}} \end{pmatrix}$$

$$= \begin{pmatrix} \prod_{\hbar=1}^{\kappa+1}\left(\mathbb{sim}\left(\frac{\pi}{2}\tilde{\rho}'_{\wp v(\hbar)}\right)\right)^{\sigma_\hbar}, \\ 1-\prod_{\hbar=1}^{\kappa+1}\left(\mathbb{sim}\left(\frac{\pi}{2}1-\tau'_{\wp v(\hbar)}\right)\right)^{\sigma_\hbar}, \\ 1-\prod_{\hbar=1}^{\kappa+1}\left(\mathbb{sim}\left(\frac{\pi}{2}1-\tilde{n}'_{\wp v(\hbar)}\right)\right)^{\sigma_\hbar} \end{pmatrix}$$

When $n = z+1$, Eq. (2) grasps for any n. The proof is finished.

Doi: https://doi.org/10.54216/IJNS.240208
Received: December 29, 2023 Revised: February 19, 2024 Accepted: April 12, 2024

(1) Consider $\mathcal{U}_{\hbar} = \{\tilde{\rho}_{\wp_{\hbar}}, \daleth_{\wp_{\hbar}}, \tilde{n}_{\wp_{\hbar}}\} \in SVNN(\beth)(\hbar = 1,2,3,\dots,n)$ in order that$\mathcal{U}_{\hbar} = \mathcal{U}$. If

$ST-SVNHWG(\mathcal{U}_1, \mathcal{U}_2, \dots, \mathcal{U}_n) = \mathbb{sim}(\mathcal{U})$.

(2) Let $\mathcal{U}_{\hbar} = \{\tilde{\rho}_{\wp_{\hbar}}, \daleth_{\wp_{\hbar}}, \tilde{n}_{\wp_{\hbar}}\}$, $\mathcal{U}_{\hbar}^{-} = \{\mathbb{mim}(\tilde{\rho}_{\wp_{\hbar}}), \mathbb{max}(\daleth_{\wp_{\hbar}}), \mathbb{max}(\tilde{n}_{\wp_{\hbar}})\}$ and $\mathcal{U}_{\hbar}^{+} = \{\mathbb{max}(\tilde{\rho}_{\wp_{\hbar}}), \mathbb{mim}(\daleth_{\wp_{\hbar}}), \mathbb{mim}(n_{\wp_{\hbar}})\} \in SVNN(\beth)(\hbar = 1,2,3,\dots,n)$. At that point,

$\mathbb{sim}(\mathcal{U}_{\hbar}^{-}) \leq ST-SVNHWG(\mathcal{U}_1, \mathcal{U}_2, \dots, \mathcal{U}_n) \leq \mathbb{sim}(\mathcal{U}_{\hbar}^{+})$.

(3) $Let\mathcal{U}_{\hbar} = \{\tilde{\rho}_{\wp_{\hbar}}, \daleth_{\wp_{\hbar}}, \tilde{n}_{\wp_{\hbar}}\}$, $\mathcal{U}_{\hbar}^{*} = \{\tilde{\rho}_{\wp_{\hbar}}^{*}, \daleth_{\wp_{\hbar}}^{*}, \tilde{n}_{\wp_{\hbar}}^{*}\} \in SVNN(\beth)(\hbar = 1,2,3,\dots,n)$. If $\tilde{\rho}_{\wp_{\hbar}} \leq \tilde{\rho}_{\wp_{\hbar}}^{*}$, $\daleth_{\wp_{\hbar}} \leq \daleth_{\wp_{\hbar}}^{*}$ and $\tilde{n}_{\wp_{\hbar}} \leq \tilde{n}_{\wp_{\hbar}}^{*}$, at that time

$ST-SVNHWG(\mathcal{U}_1, \mathcal{U}_2, \dots, \mathcal{U}_n) \leq ST-SVNHWG(\mathcal{U}_1^{*}, \mathcal{U}_2^{*}, \dots, \mathcal{U}_n^{*})$.

C. MCSA based Parameter Tuning

To improve the performance of the ISTSVNI-APP approach, the MCSA has been utilized for hyperparameter tuning of the STSVNI method. CSA is stimulated by the social behavior of crows. By considering number of crows (N_C) and dimension of problem (D), the crows of the cluster are randomly set like other metaheuristic approaches [20]. When equated to their structure of physical, crows have larger brains. Crows are considered highly intelligent birds. Depending on brain-to-body percentage, they have somewhat lesser brains than humans. Crows hide their excess food source in probably locations and once it is required they get back it. Crows often implement effective teamwork to acquire food. Hiding food sources for the next season can be a challenge for the crow since some enemies can come afterward to track the nutrition. The crow tries to fraud the enemies by changing the path in search range. Now the crow is nominated as path searches or finders and each location of crow from search range is opted as optimal point. By following and monitoring them, crows take the obscure food of another bird. Crows take several precautions like changing the obscure place to prevent becoming the next easier target.

$$Crows = \begin{bmatrix} X_1^1 & X_2^1 & \cdots & X_D^1 \\ X_1^2 & X_2^2 & \cdots & X_D^2 \\ \vdots & \vdots & \vdots & \vdots \\ X_1^{N_C} & X_2^{N_C} & \cdots & X_D^{N_C} \end{bmatrix} \quad (3)$$

At initial iteration, crows are very less qualified. Hence, they have hidden the food source in the first location. The crow's memory (M) was set by:

$$Memory = \begin{bmatrix} M_1^1 & M_2^1 & \cdots & M_D^1 \\ M_1^2 & M_2^2 & \cdots & M_D^2 \\ \vdots & \vdots & \vdots & \vdots \\ M_1^{N_C} & M_2^{N_C} & \cdots & M_D^{N_C} \end{bmatrix} \quad (4)$$

The crows upgrade the location with the cooperation of another crow. The i^{th} crow find out their feed source by examining and pursuing other crows (j^{th}). The j^{th} crow tries to cheat i^{th} crows by moving the food place under the searching range with awareness of being tracked by the enemy. The mathematical model of changing the crow's position is depicted in Eq. (5).

$$X_{new}^{i} = \begin{cases} X_{old}^{i} + r \times fl^{i} \times (M^{j} - X_{old}^{i}) r_1 \geq AP \\ LB + (UB - LB) \times rand\ Otherwise \end{cases} \quad (5)$$

In Eq. (13), two randomly produced values in the range of [0,1] are r and r_1. The awareness probability of crow indicates AP. A smaller value of AP expands the search and the maximum rate of AP expands the exploitation. The memory of crow was upgraded at every iteration with the optimum location of equivalent crows as follows:

$$M_{new}^{i} = \begin{cases} X_{new}^{i} f(X_{new}^{i}) \geq f(M_{old}^{i}) \\ M_{old}^{i}\ Otherwise \end{cases} \quad (6)$$

CSA is categorized into state-l and state-2 based on (AP) Awareness Probability. In state-l (without AP), the i^{th} crows (X_i) is following j^{th} crows (X_j), but X_j is unaware of it viz., $r_1 \geq AP$. Hence, as shown in Eq. (5). the location of X_i can be updated by conceding food location of j^{th} crows(M_j). X_i is upgraded by yielding M_j that has worst fitness values. Using this technique, the solution diverges away from the optimum solution. The entire cluster of crows is divided into smaller sets. The leader is selected by considering best crow of corresponding cluster and the followers of that cluster are upgraded by yielding the leader crow.

Doi: https://doi.org/10.54216/IJNS.240208
Received: December 29, 2023 Revised: February 19, 2024 Accepted: April 12, 2024

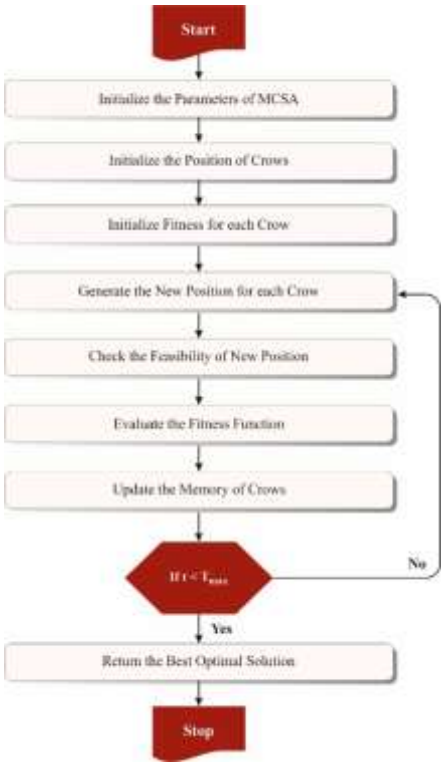

Figure 2: Flowchart of MCSA

$$X_{new}^{i} = X_{old}^{i} + r \times fl^{i} \times \left(X_{L}^{k} - X_{old}^{i}\right), If r_1 \geq AP \; k = 1,2,\cdots,ng \tag{7}$$

In Eq. (7), ng denotes the number of groups. As characterized in Eq. (8) crows are disbursed among groups by considering the weight (W),

$$W^{i} = \exp\left(-D\frac{f(X^{i}) - f(X^{Best})}{\sum_{i}^{Nc} f\,(X^{i}) - f(X^{Best})}\right) \tag{8}$$

The weight (W) is defined for rearranging the crows within [0, 1]. 0 represents worst fitness value and 1 is crow with best fitness. The followers are spread amongst the clusters by allowing the crow weight. Eqs. (9) & (10) characterize the mathematical modelling of crows in one cluster.

$$\alpha^{i} = \frac{W_{i}^{c}}{\sum_{i=1}^{ng} W_{i}^{G}} \tag{9}$$

$$N_{G_i} = round\left(\alpha^{i} \times N_{f}\right) \tag{10}$$

Where weight of leader in the group, number of crows in cluster, and amount of follower crows are W_{i}^{G}, N_{G_i}, and N_f correspondingly. Using this process, the exploitation ability can be improved. As shown in Eq. (5), when X_j is aware of its followers X_i viz., $r_1 < AP$ then i^{th} crows (X_i) are restored by arbitrarily produced crow in state-2 (with AP). It is possible that X_i is detached by the randomly produced crow with value of worst. In later iteration, the possibility of replacing best X_i by randomly produced crow with worst fitness is higher. By integrating dual arbitrary crows (X_a and X_b) and the finest crow (X_{best}) of entire group of crows, this state of CSA can be modified. The best crow of iteration estimated. The finest crow is the arbitrarily selected crow amongst the best crows attained up to now.

$$X_{new}^{i} = \begin{cases} X_{old}^{i} + r \times (X_a - X_b) + r(X_{Besf}^{m} - X_{old}^{i}) \; iff(X_a) < f(X_b) \\ X_{old}^{i} + r \times (X_b - X_a) + r(X_{Besf}^{m} - X_{old}^{i}) \; iff(X_b) < f(X_a) \end{cases} \tag{11}$$

Where the randomly selected optimal crow (viz., $m = I, 2, \ldots, it0$) is $m.\; it$ denotes the existing iteration. Fig. 2 defines the flowchart of MCSA.

Doi: https://doi.org/10.54216/IJNS.240208
Received: December 29, 2023 Revised: February 19, 2024 Accepted: April 12, 2024

The MCSA progresses a fitness function (FF) to realize greater efficacy of classifier. It defines a positive number to signify the good solution of candidate outcome. Throughout this case, the decrease of the classifier rate of error is supposed that FF, as provided in Eq. (12).

$$fitness(x_i) = ClassifierErrorRate(x_i)$$
$$= \frac{No.of\ misclassified\ samples}{Total\ no.of\ samples} * 100 \quad (12)$$

4. Experimental Validation

The AQI detection outcome of the ISTSVNI-APP technique are tested using the AQI database encompassing 1000 samples with 5 classes as depicted in Table 1. The dataset contains a number of attributes namely PM2.5, NH3, PM10, NO, SO2, NO2, NOx, CO, O3, Benzene, and toluene levels.

Table 1: Details of dataset

Classes	No. of Count
Severe	200
Moderate	200
Very Poor	200
Poor	200
Satisfactory	200
Total Count	1000

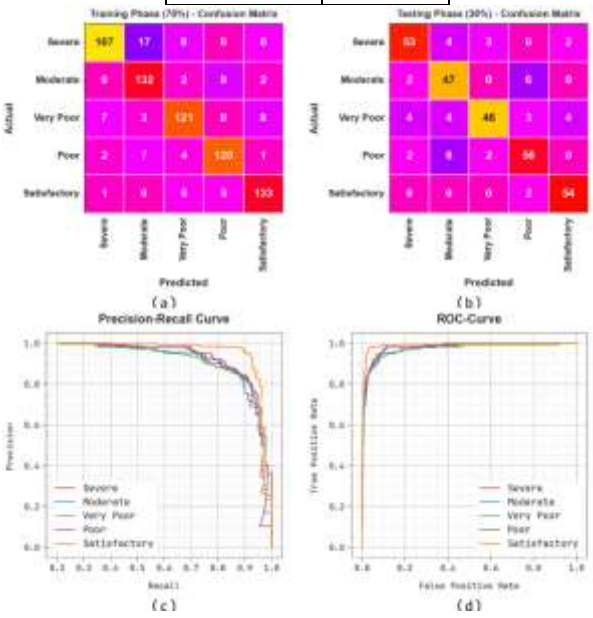

Figure 3: (a-b) 70% and 30% of confusion matrices and (c-d) PR and ROC curves

Fig. 3 illustrates the classifier performances of the ISTSVNI-APP methodology under test database. Figs. 3a-3b portrays the confusion matrices attained by the ISTSVNI-APP algorithm on 70%TRAS:30% TESS. The outcome inferred that the ISTSVNI-APP methodology has classified and distinguished all 5 classes. Afterward, Fig. 3c represents the PR curve of the ISTSVNI-APP algorithm. The experimental value demonstrated that the ISTSVNI-APP model has gained higher rate of PR at 5 class labels. Eventually, Fig. 3d exemplifies the ROC curve of ISTSVNI-APP model. The outcome defined that the ISTSVNI-APP algorithm leads to accomplished results with superior rate of ROC at 5 class labels.

Doi: https://doi.org/10.54216/IJNS.240208
Received: December 29, 2023 Revised: February 19, 2024 Accepted: April 12, 2024

The AQI detection outcomes of the ISTSVNI-APP algorithm are tested with respect to various measures in Table 2 and Fig. 4. The outcome defined that the ISTSVNI-APP approach has resulted in improved performance. On 70%TRAS, the ISTSVNI-APP technique gains average $accu_y$, $prec_n$, $reca_l$, F_{score}, and MCC of 95.03%, 87.82%, 87.51%, 87.51%, and 84.52%, correspondingly. Additionally, on 30%TESS, the ISTSVNI-APP algorithm reaches average $accu_y$, $prec_n$, $reca_l$, F_{score}, and MCC of 94.13%, 85.54%, 85.53%, 85.33%, and 81.82%, correspondingly.

Table 2: AQI detection outcome of ISTSVNI-APP technique under 70%TRAS and 30%TESS

Classes	$Accu_y$	$Prec_n$	$Reca_l$	F_{Score}	MCC
TRAS (70%)					
Severe	94.14	91.45	77.54	83.92	80.78
Moderate	94.29	83.02	91.03	86.84	83.35
Very Poor	94.71	86.43	87.05	86.74	83.44
Poor	96.00	89.55	89.55	89.55	87.08
Satisfactory	96.00	88.67	92.36	90.48	87.98
Average	95.03	87.82	87.51	87.51	84.52
TESS (30%)					
Severe	94.33	86.89	85.48	86.18	82.62
Moderate	92.67	77.05	85.45	81.03	76.66
Very Poor	93.33	90.20	75.41	82.14	78.56
Poor	93.00	83.58	84.85	84.21	79.72
Satisfactory	97.33	90.00	96.43	93.10	91.54
Average	94.13	85.54	85.53	85.33	81.82

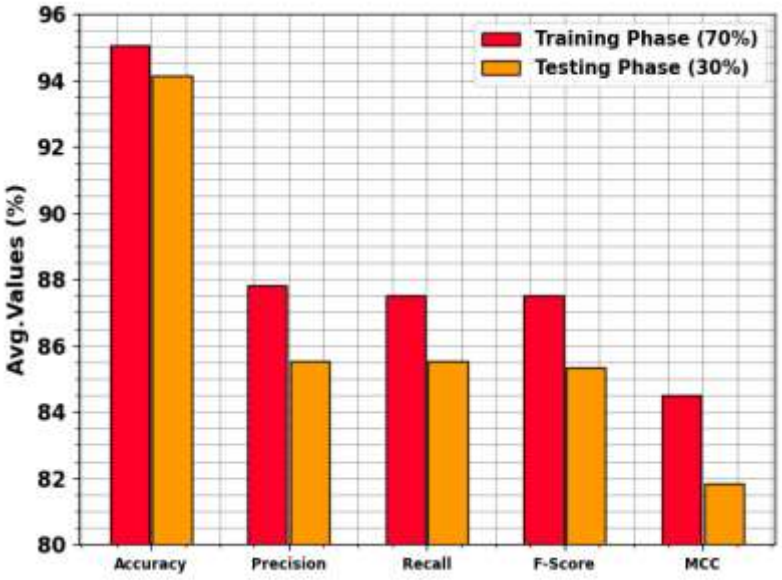

Figure 4: Average of ISTSVNI-APP technique under 70%TRAS and 30%TESS

Doi: https://doi.org/10.54216/IJNS.240208
Received: December 29, 2023 Revised: February 19, 2024 Accepted: April 12, 2024

Figure 5: $Accu_y$ curve of the ISTSVNI-APP technique

The performance of the ISTSVNI-APP approach is clearly defined in Fig. 5 in the procedure of training accuracy (TRAA) and validation accuracy (VALA) curves. The outcome depicts a functional interpretation of the behaviour of ISTSVNI-APP system under different numbers of epochs, exposing its learning model and generalized abilities. Noticeably, the outcome supposes a constant improvement from TRAA and VALA with growth in epochs. It makes sure the adaptive nature of the ISTSVNI-APP system in the pattern detection method on both data. The rising trend in VALA frameworks is the ability of the ISTSVNI-APP algorithm to adjust to the TRA data and also excel in contributing accurate classification of unnoticed data, recognizing the robust generalized proficiencies.

Fig. 6 reveals a comprehensive depiction of the training loss (TRLA) and validation loss (VALL) curve of the ISTSVNI-APP algorithm over various epochs. The continuous decline in TRLA highlights the ISTSVNI-APP system optimizing the weights and minimalizing the classifier error on both data. The outcome stated good knowledge of the ISTSVNI-APP approach associated with TRA data, emphasizing its ability to capture outlines from both data. Notable, the ISTSVNI-APP methodology constantly enhances its parameters in decreasing the variances among the predictive and real TRA classes.

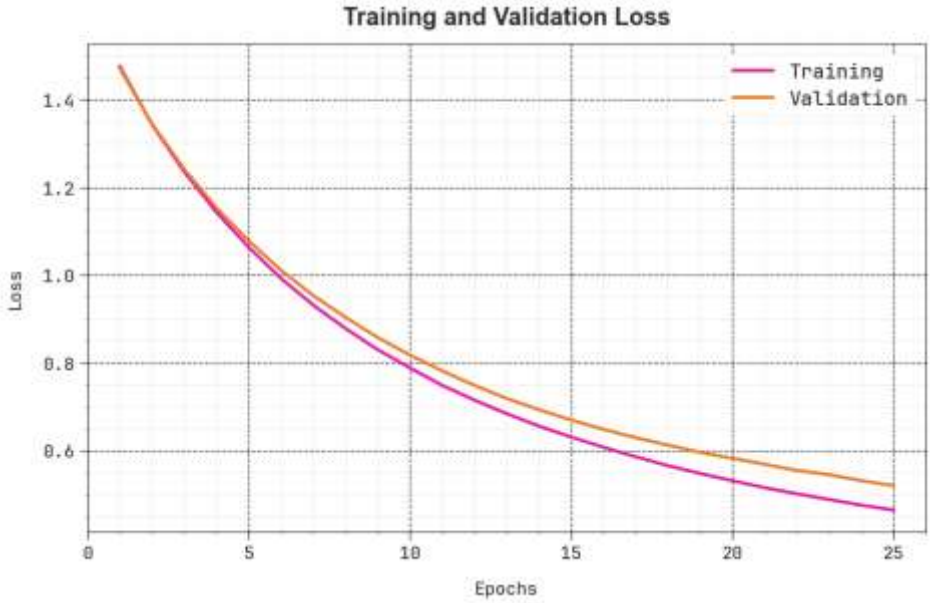

Figure 6: Loss curve of the ISTSVNI-APP technique

Doi: https://doi.org/10.54216/IJNS.240208
Received: December 29, 2023 Revised: February 19, 2024 Accepted: April 12, 2024

Table 3 displays the overall comparison outcomes of the ISTSVNI-APP methodology with other existing methods [21].

In Fig. 7, the comparative outcome of the ISTSVNI-APP model interms of $accu_y$ is reported. The figure highlighted that the ISTSVNI-APP technique gains better performance. Based on $accu_y$, the ISTSVNI-APP technique offers increased $accu_y$ of 95.03% whereas the NB, SVM, ANN, DT, SVR, RFR, and CBR models obtain decreased $accu_y$ of 86.66%, 92.40%, 93.00%, 91.99%, 92.33%, 92.98%, and 93.48%, correspondingly.

In Fig. 8, the comparative examination of the ISTSVNI-APP system with respect to $prec_n$, $reca_l$, and F_{score} is reported. The outcome exhibited that the ISTSVNI-APP system achieves optimum performance. Based on $prec_n$, the ISTSVNI-APP technique offers increased $prec_n$ of 87.82% whereas the NB, SVM, ANN, DT, SVR, RFR, and CBR approaches attain lower $prec_n$ of 72.43%, 85.59%, 84.56%, 74.96%, 86.56%, 71.37%, and 78.20%, correspondingly. Besides, based on $reca_l$, the ISTSVNI-APP method offers maximal $reca_l$ of 87.51% whereas the NB, SVM, ANN, DT, SVR, RFR, and CBR algorithms obtain minimal $reca_l$ of 70.93%, 79.73%, 75.44%, 72.56%, 70.74%, 85.74%, and 81.22%, correspondingly. Finally, based on F_{score}, the ISTSVNI-APP system offers supeiror F_{score} of 87.51% whereas the NB, SVM, ANN, DT, SVR, RFR, and CBR models obtain lower F_{score} of 82.15%, 78.09%, 77.16%, 71.64%, 71.42%, 83.31%, and 83.69%, correspondingly. Therefore, the ISTSVNI-APP technique can be applied for enhanced AQI detection results.

Table 3: Comparative analysis of ISTSVNI-APP technique with recent models

Algorithm	$Accu_y$	$Prec_n$	$Reca_l$	F_{Score}
Naïve Bayes	86.66	72.43	70.93	82.15
Support Vector Machine	92.40	85.59	79.73	78.09
Artificial neural network	93.00	84.56	75.44	77.16
Decision tree	91.99	74.96	72.56	71.64
Support Vector Regression	92.33	86.56	70.74	71.42
Random forest Regression	92.98	71.37	85.74	83.31
CatBoost Regression	93.48	78.20	81.22	83.69
ISTSVNI-APP	95.03	87.82	87.51	87.51

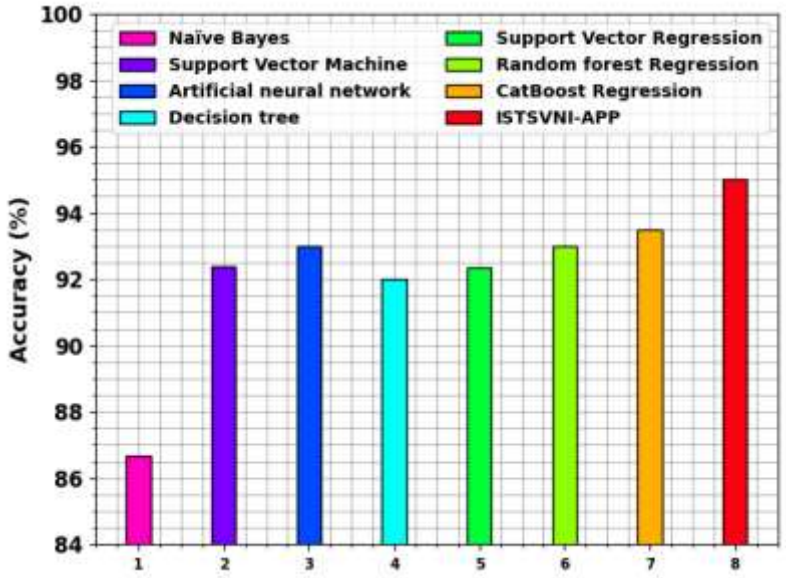

Figure 7: $Accu_y$ outcome of ISTSVNI-APP approach with recent models

Doi: https://doi.org/10.54216/IJNS.240208
Received: December 29, 2023 Revised: February 19, 2024 Accepted: April 12, 2024

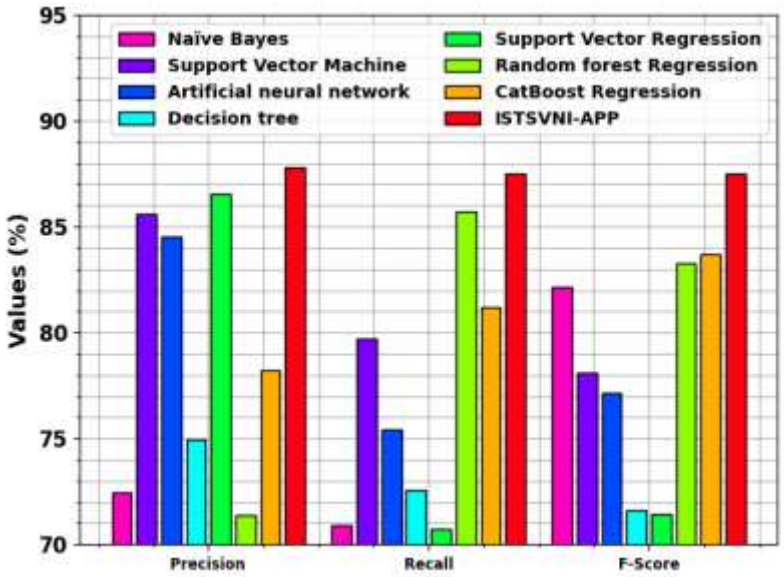

Figure 8: Comparative outcome of ISTSVNI-APP algorithm with recent systems

5. Conclusion

In this study, we have projected a novel ISTSVNI-APP model. The major objective of the ISTSVNI-APP system is to exploit AI concepts with NS models for the forecasting of air pollution. It comprises three different procedures involving min-max normalization, STSVNI based air pollution prediction, and MCSA-based parameter tuning. At the initial preprocessing step, the ISTSVNI-APP technique makes use of min-max normalization. For predicting air pollution, the ISTSVNI-APP technique uses STSVNI approach. To better the performance of the ISTSVNI-APP model, the MCSA has been deployed for hyperparameter tuning of the STSVNI system. The simulation evaluation of ISTSVNI-APP algorithm is verified utilizing a benchmark database. The experimentation outcomes stated that the ISTSVNI-APP model gains better performance in predicting air pollution.

Funding: "This project is sponsored by Prince Sattam Bin Abdulaziz University (PSAU) as part of funding for its SDG Roadmap Research Funding Programme project number PSAU-2023- SDG -59"

Conflicts of Interest: "The authors declare no conflict of interest."

References

[1] C. R. Aditya, C. R. Deshmukh, N. D K, P. Gandhi, and V. astu, "Detection and prediction of air pollution using machine learning models," International Journal of Engineering Trends and Technology, vol. 59, no. 4, pp. 204–207, 2018.

[2] H. Liu, Q. Li, D. Yu, and Y. Gu, "Air quality index and air pollutant concentration prediction based on machine learning algorithms," Applied Sciences, vol. 9, p. 4069, 2019.

[3] M. Castelli, F. M. Clemente, A. Popovic, S. Silva, and L. Vanneschi, "A machine learning approach to predict air quality in California," Complexity, vol. 2020, Article ID 8049504, 23 pages, 2020.

[4] A. Shishegaran, M. Saeedi, A. Kumar, and H. Ghiasinejad, "Prediction of air quality in Tehran by developing the nonlinear ensemble model," Journal of Cleaner Production, vol. 259, Article ID 120825, 2020.

[5] L. Tuan-Vinh, "Improving the awareness of sustainable smart cities by analyzing lifelog images and IoT air pollution data," in Proceedings of the 2021 IEEE International Conference on Big Data (Big Data), IEEE, Orlando, FL, USA, September 2021.

[6] G. Mani, J. K. Viswanadhapalli, and A. A. Stonie, "Prediction and forecasting of air quality index in Chennai using regression and ARIMA time series models," Journal of Engineering Research, vol. 9, 2021.

[7] S. V. Kottur and S. S. Mantha, "An integrated model using Artifcial Neural Network (ANN) and Kriging for forecasting air pollutants using meteorological data," Int. J. Adv. Res. Comput. Commun. Eng, vol. 4, pp. 146–152, 2015.

[8] H. Maleki, A. Sorooshian, G. Goudarzi, Z. Baboli, Y. Tahmasebi Birgani, and M. Rahmati, "Air pollution prediction by using an artifcial neural network model," Clean Technologies and Environmental Policy, vol. 21, no. 6, pp. 1341–1352, 2019

Doi: https://doi.org/10.54216/IJNS.240208
Received: December 29, 2023 Revised: February 19, 2024 Accepted: April 12, 2024

[9] S. Halsana, "Air quality prediction model using supervised machine learning algorithms," International Journal of Scientifc Research in Computer Science, Engineering and Information Technology, vol. 8, pp. 190–201, 2020.
[10] A. G. Soundari, J. Gnana, and A. C. Akshaya, "Indian air quality prediction and analysis using machine learning," International Journal of Applied Engineering Research, vol. 14, p. 11, 2019.
[11] Deepan, S. and Saravanan, M., 2024. Air quality index prediction using seasonal autoregressive integrated moving average transductive long short-term memory. ETRI Journal, p.e12658.
[12] Alkabbani, H., Ramadan, A., Zhu, Q. and Elkamel, A., 2022. An improved air quality index machine learning-based forecasting with multivariate data imputation approach. Atmosphere, 13(7), p.1144.
[13] Anggraini, T.S., Irie, H., Sakti, A.D. and Wikantika, K., 2024. Machine learning-based global air quality index development using remote sensing and ground-based stations. Environmental Advances, 15, p.100456.
[14] Van, N.H., Van Thanh, P., Tran, D.N. and Tran, D.T., 2023. A new model of air quality prediction using lightweight machine learning. International Journal of Environmental Science and Technology, 20(3), pp.2983-2994.
[15] Veeranjaneyulu, R., Boopathi, S., Kumari, R.K., Vidyarthi, A., Isaac, J.S. and Jaiganesh, V., 2023, May. Air quality improvement and optimisation using machine learning technique. In 2023 International Conference on Advances in Computing, Communication and Applied Informatics (ACCAI) (pp. 1-6). IEEE.
[16] Zhao, Z., Wu, J., Cai, F., Zhang, S. and Wang, Y.G., 2023. A hybrid deep learning framework for air quality prediction with spatial autocorrelation during the COVID-19 pandemic. Scientific Reports, 13(1), p.1015.
[17] Abirami, G., Girija, R., Das, A. and Sreenivasan, N., 2022. Predicting air quality index with machine learning models. In Machine Learning and Deep Learning in Efficacy Improvement of Healthcare Systems (pp. 353-371). CRC Press.
[18] Islam, M.J., Ahmad, S., Haque, F., Reaz, M.B.I., Bhuiyan, M.A.S. and Islam, M.R., 2022. Application of min-max normalization on subject-invariant EMG pattern recognition. IEEE Transactions on Instrumentation and Measurement, 71, pp.1-12.
[19] Ashraf, S. and Abdullah, S., 2020. Decision support modeling for agriculture land selection based on sine trigonometric single valued neutrosophic information. International Journal of Neutrosophic Science (IJNS), 9(2), pp.60-73.
[20] Das, S., Sahu, T.P. and Janghel, R.R., 2022. Stock market forecasting using intrinsic time-scale decomposition in fusion with cluster based modified CSA optimized ELM. Journal of King Saud University-Computer and Information Sciences, 34(10), pp.8777-8793.
[21] Gupta, N.S., Mohta, Y., Heda, K., Armaan, R., Valarmathi, B. and Arulkumaran, G., 2023. Prediction of air quality index using machine learning techniques: a comparative analysis. Journal of Environmental and Public Health, 2023, pp.1-26.

Doi: https://doi.org/10.54216/IJNS.240208
Received: December 29, 2023 Revised: February 19, 2024 Accepted: April 12, 2024